Hybrid Lipids as a Biological Surface-Active Component

R. Brewster,[†] P. A. Pincus,[‡] and S. A. Safran[†*]
[†]Weizmann Institute of Science, Department of Materials and Interfaces, Rehovot, Israel; and [‡]Materials Research Laboratory, University of California, Santa Barbara, California

ABSTRACT Cell membranes contain small domains (on the order of nanometers in size, sometimes called rafts) of lipids whose hydrocarbon chains are more ordered than those of the surrounding bulk-phase lipids. Whether these domains are fluctuations, metastable, or thermodynamically stable, is still unclear. Here, we show theoretically how a lipid with one saturated hydrocarbon chain that prefers the ordered environment and one partially unsaturated chain that prefers the less ordered phase, can act as a line-active component. We present a unified model that treats the lipids in both the bulk and at the interface and show how they lower the line tension between domains, eventually driving it to zero at sufficiently large interaction strengths or at sufficiently low temperatures. In this limit, finite-sized domains stabilized by the packing of these hybrid lipids can form as equilibrium structures.

INTRODUCTION

Systems capable of forming stable, finite-size domains are of biological importance in the context of membrane rafts where it has been observed that certain cellular functions are mediated by small (nanometric to tens of nanometers) domains with specific lipid composition that differs from the average composition of the membrane (1–3). These small domains are composed mainly of lipids with completely saturated hydrocarbon tails that show good orientational order in the membrane. The surrounding phase consists mostly of lipids with at least one unsaturated bond in the hydrocarbon tails, which forces a kink in the chain and inhibits chain ordering. In model systems with only two or three components (saturated lipid, unsaturated lipid, and cholesterol), this phase separation can be replicated (4,5); however, the finite domains coarsen into macroscopic domains with time (6) due to the energetic cost (line tension) of the interface between the two liquid-like phases (7). This line tension can be measured through several different techniques (8–10) and may be understood microscopically as resulting from both hydrophobic (11,12) and chain ordering mismatch at the boundary between domains. There is a large body of work dedicated to understanding phenomena such as membrane budding and fission (7,13–16) as well as membrane-shape transitions (17) as they relate to the interfacial tension between domains. Despite the importance of the line tension and the apparent small size of these domains in cellular membranes, their nature as concentration fluctuations, metastable states due to slow coarsening (18), or thermodynamically stable phases, remains unclear. In this article, we focus on the role of a particular lipid, which is soluble in the equilibrium phases but also interfacially active. We show how this lipid can lower the line tension to zero; at the same time, the hybrid lipid has only minor effects on the thermodynamics (phase diagram, critical temperature, etc.) of the system. Other factors, such as membrane recycling (19,20), cytoskeleton compartmentalization (21,22), and critical fluctuations (23,24), may also play a role in the creation and maintenance of finite-sized domains. However, the presence of a line-active component in the cell membrane can stabilize domains of a particular size over biologically useful timescales.

One particularly well-known example of finite domain formation in thermodynamic equilibrium is that of the microemulsion. Here, small drops of water can be stabilized in oil (or vice versa) by the addition of a surface active component, or surfactant, whose intermolecular interactions are most favorable at the interface between water and oil. Small concentrations of surfactant drastically reduce the surface tension at the boundaries and in some cases, can eventually drive it to zero; the creation of water-oil interface is actually energetically favored by the system because the line tension between domains is roughly zero. Our model shows how a surfactant analogy can be made for a specific lipid, referred to here as a hybrid lipid, which has one fully saturated hydrocarbon chain and one partially unsaturated chain, which are quite common in living cells (25–28). Common lipids used in model systems that have such hybrid character include POPC and SOPC. We show that when hybrid lipid is added to the typical saturated/unsaturated/cholesterol system, the hybrid preferentially absorbs to the interface between the two coexisting bulk phases—one composed mostly of saturated lipid, and the other composed mostly of the unsaturated lipid. The presence of the hybrids at the interface can have a strong effect on the interfacial tension. It is clear from experiment that the distinction between unsaturated and hybrid lipid is significant; even in the simple three-component model systems of hybrid/saturated/cholesterol, the domain size and phase behavior is not clear (5,6,29–31). Finally, while we focus on this particular class of lipid, it is also worth noting that other biological components, such as certain proteins (32,33), may also have this amphiphilic

Submitted April 1, 2009, and accepted for publication May 26, 2009.

*Correspondence: sam.safran@weizmann.ac.il

Editor: Reinhard Lipowsky.

0006-3495/09/08/1087/8 $2.00

doi: 10.1016/j.bpj.2009.05.051

property and assist in domain formation. A biological surfactant analogy has been qualitatively discussed previously (3,34) but, to our knowledge, never explored from a quantitative perspective.

As is standard in theories of lipid interactions (35,36), the interactions between lipid components are taken to depend only on the spatial ordering of their hydrocarbon chains. The various intermolecular forces are assumed to constrain packing of the chain segments at constant density inside the bilayer. Thus, the effective interaction energies considered here are the result of chain packing (entropic) considerations (36–38); such models have been successful in reproducing phase diagrams of model systems (39,40) without hybrid lipids. We characterize the degree of order by the parameter δ with a simple model of these interactions that considers a bond in the saturated chain as being either ordered $\delta = 1$ (*trans*) or disordered $\delta = 0$ (*gauche*). The unsaturated chains are taken to always be in the disordered $\delta = 0$ state, due to their chemical nature. We have ignored the differences between disordering due a permanent double bond in an unsaturated chain and a temporary *gauche* configuration of the saturated lipid. Therefore, the saturated lipids will be characterized by their local average ordering which, due to thermal effects, can range between the two extremes of being perfectly well ordered with $\delta = 1$ or as disordered as the unsaturated lipids with $\delta = 0$. The interactions between two saturated lipids is assumed to depend linearly on the local ordering parameter δ such that $J_{ss} = J\ (1 + \alpha\delta)$ (where $J_{ss} > 0$ corresponds to attractive interactions). The unsaturated lipid interactions are identical to those of the saturated lipids with $\delta = 0$, and thus $J_{uu} = J$. The mixed interaction of a saturated lipid with an unsaturated lipid is written $J_{su} = J\ (1 - \beta\delta)$; this is to say that when $\delta = 0$, once again the saturated and unsaturated lipid are identical, and when $\delta > 0$, the interactions are less favorable due to the incompatibility in lipid chain ordering that leads to steric constraints that reduce the effectiveness of the packing. The parameter J corresponds to the effective energy, resulting from the entropy loss of packing the unsaturated lipid components and serves as the energy scale for interactions. In numerical studies of chain packing interactions, it was found that an interaction strength of roughly 0.1 k_bT per c-c bond was required to match the main-chain transition temperature (41). This corresponds to a value for our interaction parameters that can range between several k_bT for short chains and between 10 and 20 k_bT for very long chains, once the coordination of the lattice is considered. The parameter α represents the entropic benefit of ordering on interacting saturated lipids whereas β represents the entropic cost of a mismatch between ordering in interacting saturated-unsaturated lipids. All three of these interaction parameters (J, α and β) are assumed to be positive. In experimental systems, these parameters can be controlled by varying the chain length of both the saturated and unsaturated lipids and degree of unsaturation or position of the double bond (42) in the unsaturated lipids. We assume that the role of cholesterol is to enhance the ordering (43,44) of either phase, and the cholesterol is therefore not explicitly included. Finally, the system includes a small concentration of hybrid lipid which, as previously mentioned, has one fully saturated hydrocarbon chain and one chain which is at least partially unsaturated (such as POPC or SOPC). The two dissimilar chains will be treated as identical to those of the saturated and unsaturated lipids; that is to say, if a hybrid lipid sits in a completely saturated environment, the total interaction is $\frac{1}{2}J_{ss} + \frac{1}{2}J_{su}$. This property means that it is energetically favorable for the hybrid lipid to occupy the interface between saturated and unsaturated lipid bulk phases and is, therefore, directly analogous to a surfactant.

SATURATED-UNSATURATED PHASE SEPARATION

Our model considers a lattice that is fully populated with saturated lipids, s, and unsaturated lipids, u. As previously mentioned, the nearest neighbor, two-body interactions between the lipids, are denoted by J_{ss} for s-s interactions, J_{uu} for u-u interactions, and J_{su} for s-u interactions, where the J parameters represent the strength of the attractive interaction between the various components and are defined more explicitly in the previous paragraph. We add to the system a small concentration of the hybrid lipid, h. The hybrid molecule occupies the bonds between lattice sites, as in Fig. 1. Each side of the hybrid molecule acts with half of the bare

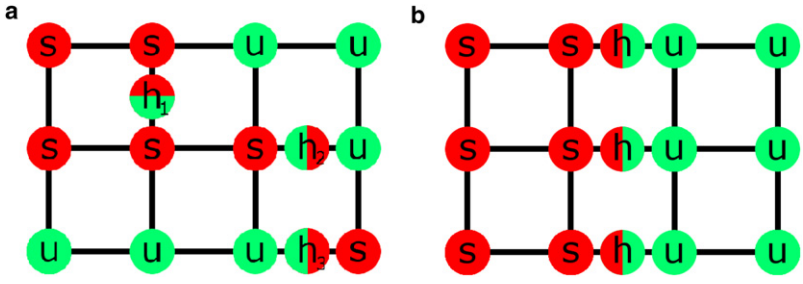

FIGURE 1 Schematic picture of (*a*) high and (*b*) low temperature (or, respectively, small/large interaction strengths, J_T) for the lattice populated with s and u molecules with some bonds occupied by the h component in various configurations. In panel *a*, the molecule labeled h_1 has the same type of neighbor on both sides and so its orientation does not matter. The two possible orientations in the presence of a concentration gradient are shown with h_2 and h_3, where h_2 is in the higher energy state, represented by orientational order parameter $\sigma = -1$. The lower energy configuration of molecule h_3 is noted by $\sigma = 1$. In the low temperature limit (*b*), entropy becomes irrelevant and the equilibrium configuration is that of lowest interaction energy where the h molecule populates the interface in the $\sigma = 1$ state.

J_{ss}, J_{uu}, or J_{su} interaction strength so that the h molecule labeled h_2 in Fig. 1 *a* does not change the total interaction energy of the system because its presence breaks one *s-u* bond and forms two half *s-u* bonds. In general, entropy dictates that the hybrid molecules are soluble in either phase and are not necessarily constrained to be located in-between an *s* and a *u* molecule (h_1 in Fig. 1 *a*). Furthermore, their orientation is not constrained to that which gives the lowest energy (h_2 in Fig. 1 *a*). Our model is similar to that of Wheeler and Widom (45) and Widom (46), with the generalization that each component is mutually soluble—an important property for these components, which can show mixed phases and critical phenomena at biologically relevant temperatures. Both the bulk and interfacial properties depend on two parameters: J_T and ΔJ. The parameter $J_T = J_{ss} + J_{uu} - 2J_{su}$ is the net interaction associated with the exchange of two *s-u* neighbors for one pair each of *s-s* and *u-u* neighbors. In terms of the molecular parameters given before, $J_T = J(\alpha + 2\beta)\delta$. When J_T is greater than zero (which is always the case so long as J, α, and β are positive) the system is capable of phase separation. The other parameter $\Delta J = J_{ss} - J_{uu} = J\alpha\delta$ represents the asymmetry in like-like interactions. In the model used here, the ordered lipids always have the most favorable interactions and therefore $\Delta J > 0$; however, this is arbitrary. Finally, for simplicity's sake, we assume that the order in the saturated chains is spatially homogeneous so that J_T and ΔJ are fixed parameters.

We calculate the mean-field free energy, phase behavior, and line tension in the Appendix for the system without hybrid. The reader can find more detailed information regarding these methods in the literature (47–49). To calculate the line tension for a wide range of interaction strengths and temperatures, we use the variational approximation described in the Appendix and shown in Fig. 2. The general result is that close to the critical temperature, the width of the interface (in the direction normal to the interface) is $\lambda = \sqrt{3/4}\xi$ and the line tension between domains (which is converted to standard units of energy/length by dividing by a^2, where a is a molecular size) is $\gamma/a = \sqrt{3J_T/T^2}(T_c - T)^{3/2}$, which are the expected, mean-field exponents that govern the correlation length and the interfacial tension. The width of the interface diverges as $\sim 1/\sqrt{T_c - T}$ and the tension goes to zero with $\sim(T_c - T)^{3/2}$ for both the linear and tanh interface shape and these physical quantities only differ by a numerical prefactor. As one increases J_T or decreases T, the tension increases indefinitely whereas the length of the interface λ decreases. In our model, we can also solve variationally for the width and free energy of the interface at large values of J_T or low temperatures. One expects, in the limit $J_T/T \to \infty$, that the interfacial width goes to its physical minimum a (the interface cannot be sharper than one lattice site) and the tension goes to J_T (the energy cost of exchanging two *s-u* bonds into a pair of *s-s* and *u-u* bonds). Indeed, these limits are recovered with our variational model up to a numeric prefactor of order unity.

SATURATED-UNSATURATED PHASE SEPARATION WITH HYBRID LIPID

We now consider the effects of adding the hybrid lipid, h, to the system. The additional term in the free energy associated with this component is

$$g_h = f_h^i + f_h^o - \mu_h\psi_h, \tag{1}$$

where f_h^i is the mean-field free energy of the hybrid lipid, which includes its entropy and interactions with the *s* and *u* lipid, and f_h^o is the free energy associated with the orientational degree of freedom of the h lipid. We denote this degree of freedom as $\sigma = \pm 1$, where $\sigma = +1$ corresponds to a hybrid lipid with its *s* tail facing an *s* lipid and its *u* tail facing a *u* lipid (such as the lipid labeled h_3 in Fig. 1 *a*) and $\sigma = -1$ corresponds to the opposite orientation. These terms can be written as

$$\begin{aligned} f_h^i = {} & T[\psi_h \log(\psi_h) + (1-\psi_h)\log(1-\psi_h)] \\ & - \frac{\psi_h}{2}\left[r_{ss}\psi^2 + r_{uu}(1-\psi)^2 + 2r_{su}\psi(1-\psi)\right], \end{aligned} \tag{2}$$

where the first term in brackets is the entropy of mixing and the next term is the essentially three-body interactions resulting from the h component occupying the space joining *s-s*, *u-u*, or *s-u* neighbors with probabilities ψ^2, $(1-\psi)^2$, and $\psi(1-\psi)$ in mean-field theory and interaction strength r_{ss}, r_{uu}, and r_{su}. Each of the three-body interaction parameters can be expressed in terms of J_T and ΔJ by $r_{ss} = -(J_T + \Delta J)/4$, $r_{uu} = -(J_T - \Delta J)/4$, and $r_{su} = J_T/4$. In this case, r_{su} simply an average over both orientations, and the orientational dependence of the interaction of an h lipid between an *s* and a *u* is corrected by a gradient term in f_h^o (50). The other contribution to the free energy is

$$f_h^o = -T\psi_h S_\sigma + \psi_h \frac{J_1\sigma(a\nabla\psi)}{2}, \tag{3}$$

where the first term is simply the entropy of the Ising parameter σ and the second term corrects for the orientational dependence of h lipids between an *s* and *u* lipid; in this case $J_1 = J_T$. In a mean-field approximation, the entropy of the orientational order parameter, σ, can be estimated by considering hybrid molecules with no interactions, but where an external field determines the orientation to have some average value $\langle\sigma\rangle$. The entropy, S_σ, is then the derivative of the partition function with respect to temperature. In an applied field v, the partition function is $z = \cosh(v/T)$. The average value of the Ising parameter is $\langle\sigma\rangle = \tanh(v/T)$ and we can solve for the entropy in terms of the average value of the Ising parameter σ. The entropy associated with the σ Ising variable is then $S_\sigma = \log[2/(1-\sigma^2)^{1/2}] - \sigma\tanh^{-1}(\sigma)$. Minimizing the free energy with respect to σ gives the free energy due to the h component $f_h = f_h^i + f_h^o$ in terms of ψ, J_T, and ΔJ:

$$f_h = T\Big[\psi_h \log(\psi_h) + (1-\psi_h)\log(1-\psi_h) - \psi_h \log\Big(\cosh\Big[\frac{J_T(a\nabla\psi)}{2T}\Big]\Big)\Big] - \frac{\psi_h}{2}\Big[J_T\psi(1-\psi) - \frac{\Delta J}{2}\Big(\psi - \frac{1}{2}\Big)\Big]. \quad (4)$$

Minimizing Eq. 2 with respect to ψ_h gives the local concentration of h lipid,

$$\psi_h = \frac{1}{1 + \exp\Big[-\dfrac{(A+\mu_h)}{T}\Big]}, \quad (5)$$

where

$$\frac{A(\psi)}{T} = \log\Big(\cosh\Big[\frac{J_T(a\nabla\psi)}{2T}\Big]\Big) + \frac{J_T}{2T}\psi(1-\psi) - \frac{\Delta J}{4T}\Big(\psi - \frac{1}{2}\Big). \quad (6)$$

The chemical potential, μ_h, is related to the total concentration of h molecules in the system by adding the local concentration in the two bulk phases, which we label + and –, and we find

$$\overline{\psi}_h = \frac{1}{2}(\psi_h^+ + \psi_h^-), \quad (7)$$

where $\overline{\psi}_h$ is the mean concentration of h lipids in the system and $\psi^{\pm}{}_h$ is the bulk phase h concentration of the two (+ and −) phases. For the special case where $\Delta J = 0$, from Eq. 7 we find $\exp(\mu_h/T) = \overline{\psi}_h \exp(-A(\psi_\infty)/T)/(1-\overline{\psi}_h)$. The parameter A compares the strength of interactions dictated by J_T/T to the chemical potential, μ_h. For small concentrations of h, μ_h is large and negative (and so is $A(\psi) + \mu_h$). In this case, $\psi_h \approx \exp[(A(\psi)+\mu_h)/T]$, which is the result for a dilute, ideal gas of h. In the limit that J_T/T dominates the μ/T contributions such that $A(\psi) + \mu_h/T$ is large and positive, $\psi_h \approx 1 - \exp[-(A(\psi)+\mu_h)/T]$. Note that, from Eqs. 5 and 6, the h molecule prefers to occupy regions of large concentration gradient. The last term in Eq. 6, proportional to $\Delta J = J_{ss} - J_{uu}$, partitions the h molecule toward whichever phase has less favorable like-like interactions, when these interactions are asymmetric.

Thermodynamics

The presence of the h amphiphile changes the thermodynamics of the system. The critical concentration will change if the interactions are asymmetric ($\Delta J \neq 0$). Because the focus of this work is to show the basic mechanism of tension reduction in the system, we will focus on the case where $\Delta J/J_T$ is small; a complete study of general ΔJ will appear in a future work. The shift in the critical concentration due to this asymmetry, $\psi_c - 1/2$, is

$$\psi_c - \frac{1}{2} = \frac{3\Delta J}{8J_T}\overline{\psi}_h, \quad (8)$$

where we have kept only linear order in $\psi_c - 1/2$ since $\Delta J/J_T \ll 1$. Of course, $\psi_c = 1/2$ for the case that the interactions are symmetric ($\Delta J = 0$ for our lattice model). The critical concentration is shifted toward systems with higher net concentrations of the more favorable component. In the bare two-component system, ΔJ had no effect on the thermodynamics. In the presence of hybrid lipids, however, ΔJ couples with the local h concentration. The physical result is that the hybrid is preferentially partitioned into the higher energy phase and lowers the total free energy. For instance, a hybrid which vacates an *s-s* bond in favor of a *u-u* bond changes the energy by $-\Delta J$, thus the hybrid will partition to the u rich phase when $\Delta J > 0$ and the s rich phase when $\Delta J < 0$; this allows the system to separate at higher concentrations of the favorable component. The critical temperature is shifted with the inclusion of hybrid lipids,

$$T_c(\overline{\psi}_h) = \frac{J_T}{4}\Big(1 - \overline{\psi}_h + \Big(\frac{\Delta J}{J_T}\Big)^2 \overline{\psi}_h\Big). \quad (9)$$

As expected, the critical temperature is an even function of ΔJ; the shift in the critical temperature cannot depend on which interaction is strongest. When $\Delta J = 0$, the critical temperature is reduced linearly with $\overline{\psi}_h$. Physically, this occurs because the h lipid stabilizes the mixed phase and inhibits phase separation. Recent work of Yethiraj and Weisshaar (51) finds the same dependence of the critical temperature on the concentration of inert, neutral spacers introduced into a lattice model of two phase-separating species. In this case, the spacers are analogous to our hybrid molecule (although they are not mobile) in that the interactions of

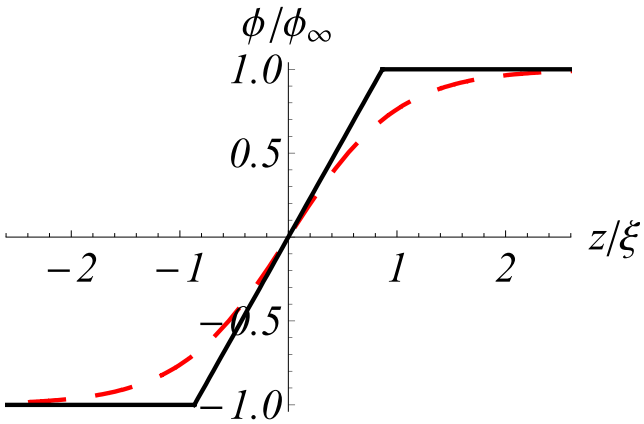

FIGURE 2 Concentration profile of the interface between the two bulk phases. The red dashed line represents the numerical solution for the continuum, mean-field expansion near T_c for the interfacial concentration that varies as $\phi \sim \tanh[z/\xi]$ and the black line is the linear approximation for the interfacial concentration profile $\phi \sim z/\lambda$ with $\lambda = \sqrt{3/4}\xi$ close to the critical temperature.

either molecule with the spacer/hybrid are more favorable than the unlike interactions (*s-u* in our case). At low spacer concentrations, the authors found that the critical temperature decreases linearly with spacer concentration. Nonzero ΔJ weakens this critical temperature reduction; however, the effect is quite small. To simplify the ensuing discussion and highlight the important features of the model, we will proceed to discuss the bulk phase behavior and tension assuming $\Delta J/J_T = 0$. A detailed treatment for general ΔJ is the subject of continuing work.

The equilibrium bulk phase concentration near the critical point is

$$\phi_\infty = \pm\sqrt{\frac{3(T_c(\overline{\psi}_h) - T)}{4T(1 - 2\overline{\psi}_h)}}, \tag{10}$$

where $\phi_\infty = \psi_\infty - \psi_c$. At the critical concentration ϕ_∞ is zero, as expected. We can also find the equilibrium bulk phase concentration in the limit where the interactions are very strong or the temperature is very low, and $\psi_\infty \approx 0$ and 1 with corrections that are exponentially small and vary as $\exp(-J_T/T)$:

$$\phi_\infty = \pm\left(\frac{1}{2} - \exp\left[\frac{-J_T}{2T}\left(1 - \frac{\overline{\psi}_h}{2}\right)\right]\right). \tag{11}$$

The presence of the *h* lipid causes the equilibrium concentrations to be somewhat larger (smaller) than their limit values close to $\psi \approx 0$ ($\psi \approx 1$), which is consistent with the result in Eq. 9 of the lowering of the critical temperature. In the different ranges of J_T or T, the hybrid (to varying degrees) inhibits phase separation.

Line tension

We now calculate the line tension associated with both the regime of weak and strong interaction strengths (temperatures near the critical point and low temperatures). We must add to the tension calculated in Eq. 16 a contribution associated with the *h* molecule. Near the critical temperature, the *h* molecules are distributed fairly uniformly with only a small concentration near the interface. In this case, the line tension is

$$\frac{\gamma}{a} = \sqrt{\left[\frac{16J_T}{3}\left(1 - \frac{J_T\overline{\psi}_h}{4T}\right)(T_c(\overline{\psi}_h) - T)\right]}\phi_\infty^2. \tag{12}$$

The form is similar to that of the bare, two-component system; however, it is clear that the presence of the *h* molecule serves to lower the surface tension (in addition to effects from the changes to the thermodynamics that result in a renormalization of the critical temperature Eq. 9 and the bulk concentrations Eq. 8). This lowering is due entirely to the gradient term in the hybrid free energy. However, in the limit that $\overline{\psi}_h$ is small, the change in the tension is small and can never go to zero; finite-sized domain formation will not be favored and macroscopic phase separation will occur.

In the large interaction strength or low temperature limits, the bulk phase concentrations are simply $\phi_\infty = \pm 1/2$ with corrections that scale as $\exp[-J_T/2T]$, which are negligible once $J_T/2T$ is larger than 3 or 4. An analytic expression for λ in this regime cannot be derived; however, it is clear that the hybrid molecule serves to sharpen the interface and decrease λ. Physically, this happens because the amphiphile prefers to occupy regions of high concentration gradients where there are many *s-u* bonds whose energy can be reduced by the *h* lipids. The interface, however, cannot be smaller than one lattice spacing, *a*. Thus, in calculating the interfacial tension in the large J_T or low temperature limit, we take $\lambda/a = 1$. Once again, from Eq. 5, the concentration of *h* at the interface is 1 with corrections proportional to $\exp(-J_T/T)$, which we ignore. Now when J_T/T is extremely large, the interfacial tension is

$$\frac{\gamma}{a} = -\frac{J_T}{4}\left(1 + \frac{4T\log(\overline{\psi}_h)}{J_T}\right). \tag{13}$$

Thus, an extrapolation of this formula suggests that the line tension goes to zero at $\overline{\psi}_h \approx \exp(-J_T/4T)$. The exact solution for the normalized line tension assuming the bulk phase concentrations are close to 0 or 1 with corrections exponential in J_T/T, with $\psi = 1/2$ at a sharp interface, is shown as the continuous curves in Fig. 3. The colored points in these figures represent the result of ignoring these exponential corrections (Eq. 13); this approach is only valid in the limit of large J_T or low T). Fig. 3 *a* shows that for even small concentrations of *h* ($\overline{\psi}_h = 0.01$ for *black solid line*, $\overline{\psi}_h = 0.05$ for *red dashed line*), the line tension indeed goes to zero at a finite value of J_T/T that agrees with the value found from Eq. 13. To estimate the tension, we note that in Fig. 3 *a* the maximum value of γ occurs at $J_T/T \approx 6$ with $\gamma = 0.25\, ak_BT$. Taking $a = 2$ nm and converting γ to standard units of energy/length by dividing by a^2, we estimate the maximum tension to be roughly 3–4 pN, consistent with the scale of tension measurements of domains in experiments (52,53). Also shown, in the inset to Fig. 3 *a*, is the local concentration of *h* molecules at the interface for these same two values of $\overline{\psi}_h$ (0.01 for *black solid line* and 0.05 for *red dashed*). The line tension goes to zero when $\psi_h \approx 1$ and the amount of hybrid at the interface is saturated. For nonzero values of ΔJ, the largest effect would likely be in altering the value of J_T/T, at which ψ_h saturates the interface. From Eqs. 5 and 6, we can extrapolate that ΔJ would serve to slow this saturation because ΔJ and $\psi - 1/2$ at the interface will always have the same sign from Eq. 8. However, for large values of J_T or for low values of T, we expect that ψ at the interface is equal to 1/2 since the bulk concentrations are very close to either zero or unity. Thus, the effect of ΔJ should disappear at high J_T or low T. Fig. 3 *b* shows the scenario that can more easily be measured in experiment where J_T/T is fixed by the chemistry and where it is feasible to vary the concentration of *h* molecules in the system. We show here that for a large

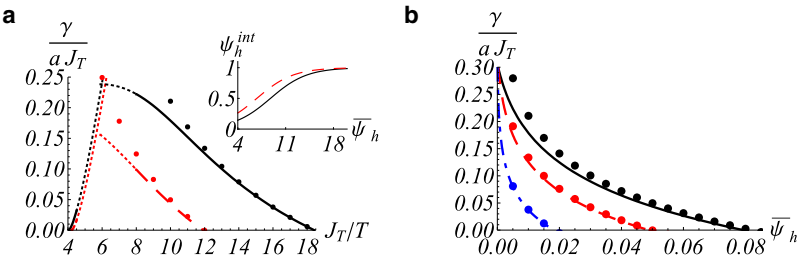

FIGURE 3 (*a*) Normalized tension versus interaction strength, J_T/T, near the critical point and for strong interaction strengths (or low temperatures) with $J_T/T \gg 1$, for which the interface thickness is a molecular length and the bulk phases are $\psi = 0$ and 1 with corrections proportional to $\exp(-J_T/T)$. The black solid line shows the normalized tension $\gamma/(aJ_T)$ for $\overline{\psi}_h = 0.01$ and the red dashed line shows the tension for $\overline{\psi}_h = 0.05$. The thin dotted lines, intermediate between the critical temperature and the low temperature (strong interaction) regime, are continuations of these solutions into the region between the two extreme regimes. The colored points, which coincide with the plots of γ for low temperatures (or strong interactions), are plots of Eq. 13, where terms proportional to $\exp(-J_T/T)$ are ignored. The presence of the *h* component at the interface drives the line tension to zero, as can be seen in the inset, which shows the interfacial concentration of *h*, ψ^{int}_h, for $\overline{\psi}_h = 0.01$ (*black solid line*) and $\overline{\psi}_h = 0.05$ (*red dashed line*). (*b*) Line tension versus average *h* concentration for a fixed interaction strength $J_T/T = 10$ (*black solid*), 12 (*red dashed*), and 16 (*blue dot-dashed*). The colored points are, again, from Eq. 13. The tension is driven to zero as $\overline{\psi}_h$, an experimentally controlled parameter, is increased. For the interaction strengths chosen, the tension reaches zero for very small concentrations of $\overline{\psi}_h$. Values of J_T include the number of nearest neighbors and the number of chains per lipid. For a linear interface, a value of $J_T/T = 16$ implies an interaction strength of ~4 *kT* per chain.

range of values of J_T/T there is a corresponding concentration of *h* for which the line tension is driven to zero. This, of course, assumes that the interactions are strong enough to provide a sharp interface between domains. It is clear that the interfacial tension can easily reach zero in this regime even for small values of $\overline{\psi}_h$. Thus, although the surfactant contributes only linearly to the thermodynamic bulk terms (e.g., shift in the critical concentration and temperature) it contributes more strongly, logarithmically, to the line tension. Furthermore, this contribution is linear in T/J_T whereas the corrections to the bulk equilibrium concentrations vary like $\exp[J_T/T] \ll T/J_T/T$ for $J_T/T \gg 1$ (high interaction strength or low temperatures).

CONCLUSIONS

In summary, we have shown how a mixture of biologically relevant lipids can stabilize the formation of finite domains. The hybrid lipids can do this by driving the line tension to zero; this occurs when the net interaction strength J_T/T is large enough to overcome the entropic gains of random mixing and orientation. The interface then becomes saturated with hybrid lipids whose molecular orientation is energetically favorable. In practice, lipids with longer chains increase the interaction strength and should more readily form finite domains. In addition, the degree of unsaturation in the unsaturated chains (or even position of the unsaturated bond(s) (42)) will affect the interaction strength; increasing the number of unsaturated bonds increases the effective difference in ordering between the two phases, which results in a net increase of J_T. Additionally, the line tension is driven to zero at higher temperatures (or lower interaction strengths) if the concentration of hybrid lipids in the system is increased. However, even low concentrations of hybrid can induce finite domain formation if the interaction strength is large enough or the temperature is low enough. Our calculations show that near the critical temperature the line tension never reaches zero for low concentrations of *h*. Several experiments can be suggested to test these predictions. For example, the fluctuations of the domain boundaries between liquid ordered and disordered phases can give a measurement of the interfacial line tension as a function of hybrid concentration (54,55). In addition, tracking labeled hybrid lipids to verify that they are indeed interfacially active would provide experimental evidence of this important characteristic. Finally, we note that while we predict the conditions under which the line tension goes to zero, the size of the domains will be determined by more detailed packing considerations. Similar to surfactant packing at an interface (47), we expect there to be a spontaneous curvature, due to the difference in area per headgroup of the two unlike alkyl chains of the hybrid lipid, which will dictate the optimal domain size. The microscopic effects that lead to this will depend on the lipid geometry and are deserving of further consideration.

APPENDIX

The mean-field thermodynamic potential per lattice spacing for the bare, two-component *s-u* system can be written as

$$g = f_0 + \frac{J_T(a\nabla\psi)^2}{4} - \mu\psi, \tag{14}$$

where

$$f_0 = T[\psi\log(\psi) + (1-\psi)\log(1-\psi)] + \frac{1}{2}[J_T\psi(1-\psi) - \Delta J\psi - J_{uu}] \tag{15}$$

is the free energy of the homogeneous phase in terms of the local concentration, ψ, of the saturated component, *s*. The first term in brackets is simply the mixing entropy and the second term is the Hamiltonian for two-body interactions. The gradient term in Eq. 14 assigns an energy cost to concentration gradients of *s* and *u* (that must be even in $\nabla\psi \rightarrow -\nabla\psi$) and the prefactor *a* is a molecular scale that fixes the gradient term to units of the lattice spacing. The chemical potential, μ, accounts for conservation of the concentration of the saturated lipid. The critical temperature and concentration are obtained from setting $\partial^2 f_0/\partial\psi^2 = 0$ and $\partial^3 f_0/\partial\psi^3 = 0$ evaluated at the critical composition. The critical concentration, then, is simply $\psi_c = 1/2$ and the

critical temperature is $T_c = J_T/4$. When the temperature is just below T_c, the system separates into two coexisting phases with composition close to the critical composition. Finally, the equilibrium phase concentrations close to the critical temperature are then $\phi_\infty = \pm\sqrt{3(T_c - T)/4T}$, where $\phi = \psi - 1/2$. In the two-component system, the thermodynamics does not depend on ΔJ; it depends only on J_T. The parameter ΔJ simply renormalizes the chemical potential.

The tension is the free energy cost of having an interface between these two bulk phases. The functional minimization of the Landau-Ginzburg expansion of Eq. 14 with the boundary conditions that the gradient vanishes at $z = \pm\infty$ yields an interfacial profile for the temperature regime close to the critical point which goes as $\phi = \phi_\infty \tanh[z/\xi]$, where $\xi = \sqrt{J_T/4(T_c - T)}$ is the width of the interface in the normal direction (47). It is difficult to solve for the interfacial concentration profile in all temperature regimes. Therefore, we use a variational approximation for the interface profile with a linear concentration variation between $z = \pm\lambda$ and $\phi = \phi_\infty z/\lambda$, where λ is the width of the interface (and not necessarily the same as ξ). The variational parameter λ is found by minimizing the tension with respect to this interfacial width λ. Finally, the concentration is $-\phi_\infty$ for $z < -\lambda$ and ϕ_∞ for $z > \lambda$. A schematic diagram of these two concentration profiles is shown in Fig. 2. A general expression for the tension with the linear concentration gradient along the interface is found by comparing the energy difference of an interface with that of bulk phase $\gamma = \int_{-\infty}^{\infty}(g(\psi) - g_b)dz$, where g_b is the thermodynamic potential of the bulk. To convert this measure of line tension (which has units of energy times length) to the physical line tension with units of energy/length, our γ must be divided by a^2. A general expression for the line tension in the two-component system in this variational approximation that is valid in the entire temperature range is

$$\frac{\gamma}{a} = T\frac{\lambda}{a}\left[-1 + \left(\frac{1}{2\phi_\infty} - 2\phi_\infty\right)\arctan[2\phi_\infty] + \frac{2J_T\phi_\infty^2}{3T}\right] + \frac{J_T a\phi_\infty^2}{2\lambda}, \tag{16}$$

and a general expression for the width of the interface follows from minimizing Eq. 16 with respect to λ. Now we only require the relationship between ϕ_∞ and J_T/T to determine both λ and γ. For our simple case where $\mu = 0$, ϕ_∞ is found by minimizing f_0 with respect to ψ.

We are grateful for discussions with M. Schick, I. Szleifer, R. Ziblat, L. Addadi, S. Veatch, S. Keller, B. Widom, L. Silva, and A. Yethiraj.

The authors acknowledge support from the U.S.-Israel Binational Science Foundation, the U.S.-Israel Educational Foundation, and an Israel Science Foundation Converging Technologies grant. This research is made possible in part by the historic generosity of the Harold Perlman family.

REFERENCES

1. Simons, K., and E. Ikonen. 1997. Functional rafts in cell membranes. *Nature*. 387:569–572.
2. Edidin, M. 2003. The state of lipid rafts: from model membranes to cells. *Annu. Rev. Biophys. Biomol. Struct*. 32:257–283.
3. Hancock, J. F. 2006. Lipid rafts: contentious only from simplistic standpoints. *Nat. Rev. Mol. Cell Biol*. 7:456–462.
4. Veatch, S. L., and S. L. Keller. 2002. Organization in lipid membranes containing cholesterol. *Phys. Rev. Lett*. 89:268101.
5. de Almeida, R. F. M., L. M. S. Loura, A. Fedorov, and M. Prieto. 2005. Lipid rafts have different sizes depending on membrane composition: a time-resolved fluorescence resonance energy transfer study. *J. Mol. Biol*. 346:1109–1120.
6. Veatch, S. L., and S. L. Keller. 2005. Seeing spots: complex phase behavior in simple membranes. *Biochim. Biophys. Acta Mol. Cell Res*. 1746:172–185.
7. Lipowsky, R. 1992. Budding of membranes induced by intramembrane domains. *J. Phys. II (Fr.)*. 2:1825–1840.
8. Benvegnu, D., and H. McConnell. 1992. Line tension between liquid domains in lipid monolayers. *J. Phys. Chem*. 96:6820–6824.
9. Goldstein, R., and D. Jackson. 1994. Domain shape relaxation and the spectrum of thermal fluctuations in Langmuir monolayers. *J. Phys. Chem*. 98:9626–9636.
10. Wurlitzer, S., P. Steffen, and T. Fischer. 2000. Line tension of Langmuir monolayer phase boundaries determined with optical tweezers. *J. Chem. Phys*. 112:5915–5918.
11. Kuzmin, P., S. Akimov, Y. Chizmadzhev, J. Zimmerberg, and F. Cohen. 2005. Line tension and interaction energies of membrane rafts calculated from lipid splay and tilt. *Biophys. J*. 88:1120–1133.
12. Akimov, S. A., P. I. Kuzmin, J. Zimmerberg, and F. S. Cohen. 2007. Lateral tension increases the line tension between two domains in a lipid bilayer membrane. *Phys. Rev. E Stat. Nonlin. Soft Matter Phys*. 75:011919.
13. Lipowsky, R. 2002. Domains and rafts in membranes—hidden dimensions of self-organization. *J. Biol. Phys*. 28:195–210.
14. Staneva, G., M. Seigneuret, K. Koumanov, G. Trugnan, and M. I. Angelova. 2005. Detergents induce raft-like domains budding and fission from giant unilamellar heterogeneous vesicles: a direct microscopy observation. *Chem. Phys. Lipids*. 136:55–66.
15. Dobereiner, H., J. Kas, D. Noppl, I. Sprenger, and E. Sackmann. 1993. Budding and fission of vesicles. *Biophys. J*. 65:1396–1403.
16. Sens, P., and M. Turner. 2006. Budded membrane microdomains as tension regulators. *Phys. Rev. E Stat. Nonlin. Soft Matter Phys*. 73:031918.
17. Jülicher, F., and R. Lipowsky. 1996. Shape transformations of vesicles with intramembrane domains. *Phys. Rev. E Stat. Phys. Plasmas Fluids Relat. Interdiscip. Topics*. 53:2670–2683.
18. Frolov, V., Y. Chizmadzhev, F. Cohen, and J. Zimmerberg. 2006. Entropic traps in the kinetics of phase separation in multicomponent membranes stabilize nanodomains. *Biophys. J*. 91:189–205.
19. Turner, M., P. Sens, and N. Socci. 2005. Nonequilibrium raftlike membrane domains under continuous recycling. *Phys. Rev. Lett*. 95:168301–168304.
20. Gomez, J., F. Sagues, and R. Reigada. 2008. Actively maintained lipid nanodomains in biomembranes. *Phys. Rev. E Stat. Nonlin. Soft Matter Phys*. 77:021907.
21. Fujiwara, T., K. Ritchie, H. Murakoshi, K. Jacobson, and A. Kusumi. 2002. Phospholipids undergo hop diffusion in compartmentalized cell membrane. *J. Cell Biol*. 157:1071–1081.
22. Murase, K., T. Fujiwara, Y. Umemura, K. Suzuki, R. Iino, et al. 2004. Ultrafine membrane compartments for molecular diffusion as revealed by single molecule techniques. *Biophys. J*. 86:4075–4093.
23. Honerkamp-Smith, A. R., P. Cicuta, M. D. Collins, S. L. Veatch, M. den Nijs, et al. 2008. Line tensions, correlation lengths, and critical exponents in lipid membranes near critical points. *Biophys. J*. 95:236–246.
24. Veatch, S. L., P. Cicuta, P. Sengupta, A. Honerkamp-Smith, D. Holowka, et al. 2008. Critical fluctuations in plasma membrane vesicles. *ACS Chem. Biol*. 3:287–293.
25. Kuksis, A., L. Marai, W. Breckenridge, D. Gornal, and O. Stachnyk. 1968. Molecular species of lecithins of some functionally distinct rat tissues. *Can. J. Phys. Pharmacol*. 46:511–524.
26. Yabuuchi, H., and J. Obrien. 1968. Positional distribution of fatty acids in glycerophosphatides of bovine gray matter. *J. Lipid Res*. 9:65–67.
27. Wood, R., and R. D. Harlow. 1969. Structural studies of neutral glycerides and phosphoglycerides of rat liver. *Arch. Biochem. Biophys*. 131:495–501.
28. Holub, B., and A. Kuksis. 1969. Molecular species of phosphatidyl ethanolamine from egg yolk. *Lipids*. 4:466–472.
29. Zhao, J., J. Wu, H. Shao, F. Kong, N. Jain, et al. 2007. Phase studies of model biomembranes: macroscopic coexistence of L_α plus L_β, with

light-induced coexistence of L_α plus L_o phases. *Biochim. Biophys. Acta Biomembr.* 1768:2777–2786.

30. Feigenson, G. W. 2007. Phase boundaries and biological membranes. *Annu. Rev. Biophys. Biomol. Struct.* 36:63–77.
31. Feigenson, G. W. 2009. Phase diagrams and lipid domains in multicomponent lipid bilayer mixtures. *Biochim. Biophys. Acta Biomembr.* 1788:47–52.
32. Nicolini, C., J. Baranski, S. Schlummer, J. Palomo, M. Lumbierres-Burgues, et al. 2006. Visualizing association of N-Ras in lipid microdomains: influence of domain structure and interfacial adsorption. *J. Am. Chem. Soc.* 128:192–201.
33. Buzhynskyy, N., J. F. Girmens, W. Faigle, and S. Scheuring. 2007. Human cataract lens membrane at subnanometer resolution. *J. Mol. Biol.* 374:162–169.
34. Lipowsky, R., and R. Dimova. 2003. Domains in membranes and vesicles. *J. Phys. Cond. Matter.* 15:S31–S45.
35. Shaul, B. A., and W. M. Gelbart. 1985. Theory of chain packing in amphiphilic aggregates. *Annu. Rev. Phys. Chem.* 36:179–211.
36. Szleifer, I., A. Ben-Shaul, and W. M. Gelbart. 1986. Chain statistics in micelles and bilayers: effects of surface roughness and internal energy. *J. Chem. Phys.* 85:5345–5358.
37. Pandit, S., D. Bostick, and M. Berkowitz. 2004. Complexation of phosphatidylcholine lipids with cholesterol. *Biophys. J.* 86:1345–1356.
38. Zhang, Z., L. Lu, and M. L. Berkowitz. 2008. Energetics of cholesterol transfer between lipid bilayers. *J. Phys. Chem. B.* 112:3807–3811.
39. Elliott, R., I. Szleifer, and M. Schick. 2006. Phase diagram of a ternary mixture of cholesterol and saturated and unsaturated lipids calculated from a microscopic model. *Phys. Rev. Lett.* 96:098101.
40. Putzel, G. G., and M. Schick. 2008. Phenomenological model and phase behavior of saturated and unsaturated lipids and cholesterol. *Biophys. J.* 95:4756–4762.
41. Elliott, R., K. Katsov, M. Schick, and I. Szleifer. 2005. Phase separation of saturated and mono-unsaturated lipids as determined from a microscopic model. *J. Chem. Phys.* 122:144904.
42. Martinez-Seara, H., T. Rog, M. Pasenkiewicz-Gierula, I. Vattulainen, M. Karttunen, et al. 2008. Interplay of unsaturated phospholipids and cholesterol in membranes: effect of the double-bond position. *Biophys. J.* 95:3295–3305.
43. Henriksen, J., A. C. Rowat, E. Brief, Y. W. Hsueh, J. L. Thewalt, et al. 2006. Universal behavior of membranes with sterols. *Biophys. J.* 90:1639–1649.
44. Pan, J., T. T. Mills, S. Tristram-Nagle, and J. F. Nagle. 2008. Cholesterol perturbs lipid bilayers nonuniversally. *Phys. Rev. Lett.* 100:198103.
45. Wheeler, J. C., and B. Widom. 1968. Phase transitions and critical points in a model 3-component system. *J. Am. Chem. Soc.* 90:3064–3071.
46. Widom, B. 1984. Lattice-gas model of amphiphiles and of their orientation at interfaces. *J. Phys. Chem.* 88:6508–6514.
47. Safran, S. A. 2003. Statistical Thermodynamics of Surfaces, Interfaces and Membranes. Westview Press, Boulder, CO.
48. Plischke, M., and B. Bergersen. 2006. Equilibrium Statistical Physics. World Scientific Publishing, Singapore.
49. Chaikin, P. M., and T. C. Lubensky. 1995. Principles of Condensed Matter Physics. Cambridge University Press, Cambridge, United Kingdom.
50. Chen, K., C. Jayaprakash, R. Pandit, and W. Wenzel. 1990. Microemulsions: a Landau-Ginzburg theory. *Phys. Rev. Lett.* 65:2736–2739.
51. Yethiraj, A., and J. C. Weisshaar. 2007. Why are lipid rafts not observed in vivo? *Biophys. J.* 93:3113–3119.
52. Baumgart, T., S. Hess, and W. Webb. 2003. Imaging coexisting fluid domains in biomembrane models coupling curvature and line tension. *Nature.* 425:821–824.
53. Tian, A., C. Johnson, W. Wang, and T. Baumgart. 2007. Line tension at fluid membrane domain boundaries measured by micropipette aspiration. *Phys. Rev. Lett.* 98:208102.
54. Stottrup, B. L., A. M. Heussler, and T. A. Bibelnieks. 2007. Determination of line tension in lipid monolayers by Fourier analysis of capillary waves. *J. Phys. Chem. B.* 111:11091–11094.
55. Esposito, C., A. Tian, S. Melamed, C. Johnson, S.-Y. Tee, et al. 2007. Flicker spectroscopy of thermal lipid bilayer domain boundary fluctuations. *Biophys. J.* 93:3169–3181.